Diagnostic Value of Diffusion-Weighted Imaging in Simultaneous ^{18}F-FDG PET/MR Imaging for Whole-Body Staging of Women with Pelvic Malignancies

Johannes Grueneisen[1], Benedikt Michael Schaarschmidt[2], Karsten Beiderwellen[1], Antonia Schulze-Hagen[3], Martin Heubner[3], Sonja Kinner[1], Michael Forsting[1], Thomas Lauenstein[1], Verena Ruhlmann[4], and Lale Umutlu[1]

[1]Department of Diagnostic and Interventional Radiology and Neuroradiology, University Hospital Essen, University of Duisburg-Essen, Essen, Germany; [2]Department of Diagnostic and Interventional Radiology, University Hospital Dusseldorf, University of Dusseldorf, Dusseldorf, Germany; [3]Department of Obstetrics and Gynecology, University Hospital Essen, University of Duisburg-Essen, Essen, Germany; and [4]Department of Nuclear Medicine, University Hospital Essen, University of Duisburg-Essen, Essen, Germany

The aim of this study was to assess the diagnostic benefit of diffusion-weighted imaging (DWI) in an ^{18}F-FDG PET/MR imaging protocol for whole-body staging of women with primary or recurrent malignancies of the pelvis. **Methods:** Forty-eight patients with a primary pelvic malignancy or suspected recurrence of a pelvic malignancy were included in our study. All patients underwent a whole-body ^{18}F-FDG PET/MR imaging examination that included DWI. Two radiologists separately evaluated the PET/MR imaging datasets without DWI followed by a second interpretation with DWI. First, both readers identified all primary tumors, as well as lymph node and distant metastases. In a second session, PET and DWI data were assessed qualitatively. Image interpretation comprised lesion conspicuity defined as visual lesion-to-background contrast (4-point ordinal scale) and diagnostic confidence (3-point ordinal scale) for all tumors. The results from histopathologic examination and cross-sectional imaging follow-up (≥6 mo) were used as the reference standard. Statistical analysis was performed to assess the significance of differences between obtained values. **Results:** Among the 122 suspected lesions seen, 98 (80.3%) were considered malignant. PET/MR imaging without DWI had a sensitivity, specificity, positive predictive value, negative predictive value, and diagnostic accuracy of 92.9%, 87.5%, 96.8%, 75.0%, and 91.8%, respectively, for the detection of malignant lesions. PET/MR imaging with DWI had slightly higher values (94.9%, 83.3%, 95.9%, 80.0%, and 92.6%, respectively), but the difference was not significant ($P > 0.05$). In the qualitative assessment of lesion-to-background contrast, PET had significantly ($P < 0.05$) higher values (3.79 ± 0.58) than DWI (3.63 ± 0.77). Furthermore, significantly ($P < 0.05$) higher scores were found for diagnostic confidence using PET (2.68 ± 0.64) for the determination of malignant lesions, when compared with DWI (2.53 ± 0.69). **Conclusion:** DWI in PET/MR imaging has no diagnostic benefit for whole-body staging of women with pelvic malignancies. The omission of DWI for staging or restaging gynecologic cancer may significantly reduce examination times, thus increasing patient comfort without a relevant decrease in diagnostic competence.

Key Words: PET/MRI; diffusion-weighted imaging; ^{18}F-FDG PET; gynecological cancers

J Nucl Med 2014; 55:1930–1935
DOI: 10.2967/jnumed.114.146886

Highly accurate oncologic staging and restaging for early detection of potential tumor sites is required to ensure appropriate patient management and increase overall patient survival. Conventional morphologic MR imaging is considered highly valuable for assessing local tumor extent and potential metastatic spread (*1,2*). Nevertheless, the introduction of diffusion-weighted imaging (DWI) as an additional functional parameter to morphologic imaging has been shown to significantly increase sensitivity for identification of tumors and metastatic sites (*3*). Furthermore, DWI has been shown to increase the specificity for characterization of suspected lesions, by quantifying the apparent diffusion coefficient (ADC), which is significantly lower in malignant lesions than in healthy parenchyma or noncancerous tissues (*4,5*). The use of integrated PET/CT has become well established within the last decade for whole-body staging in oncologic patients (*6*). Various studies investigating the diagnostic capacity of DWI or MR imaging and of PET/CT have reported comparable results for detection and characterization of tumors, including gynecologic malignancies (*7–9*).

The recent introduction of PET/MR imaging scanners has opened a new platform for simultaneous high-quality assessment of local tumor extent and metastatic spread by combining morphologic (MR imaging), functional (DWI), and metabolic (PET) features (*10–12*). Nevertheless, a distinct disadvantage of PET/MR imaging compared with PET/CT lies in the significantly prolonged examination time, caused mainly by the acquisition of a substantial number of available MR sequences. Hence, with regard to patient comfort based on a reasonable scanning duration, the need to optimize and implement suitable, well-adapted dedicated MR imaging protocols for certain tumor entities has arisen.

Therefore, with regard to shortening study protocols, the aim of this trial was to assess whether the addition of the functional parameter DWI to PET/MR imaging for whole-body staging of women with malignancies of the pelvis has potential diagnostic benefit.

Received Aug. 12, 2014; revision accepted Oct. 8, 2014.
For correspondence or reprints contact: Johannes Grueneisen, Department of Diagnostic and Interventional Radiology and Neuroradiology, University Hospital Essen, Hufelandstrasse 55, 45147 Essen, Germany.
E-mail: Johannes.grueneisen@uk-essen.de
Published online Nov. 11, 2014.

MATERIALS AND METHODS

Patients

The study was approved by the local institutional review board. Written informed consent was obtained from all patients before each examination. Forty-eight consecutive patients (mean age, 52.8 ± 11.6 y; range, 26–73 y) with a primary pelvic malignancy or suspected recurrence of a pelvic malignancy were prospectively enrolled. A total of 27 patients with histopathologically confirmed primary tumors underwent a PET/MR imaging examination before any therapeutic interventions. All patients in whom tumor recurrence was suspected ($n = 21$) had initially undergone treatment at the time of first diagnosis and had been considered disease-free during follow-up examinations for a minimum of 6 mo before PET/MR imaging. The inclusion criteria encompassed histopathologic confirmation of disease recurrence as well as clinical follow-up examinations and cross-sectional imaging follow-up of more than 6 mo after PET/MR imaging examinations.

PET/MR Imaging

Whole-body PET/MR imaging examinations were performed on a 3-T Biograph mMR (Siemens Healthcare), using lutetium oxyorthosilicate–based photodiodes for the acquisition of PET datasets. Patients with primary tumors underwent only PET/MR imaging (2 MBq/kg of body weight), whereas patients with recurrent tumors underwent first clinically indicated PET/CT and then PET/MR imaging (4 MBq/kg of body weight). PET/MR imaging scans started at an average delay of 93 ± 36 min after intravenous ^{18}F-FDG administration, resulting in a mean activity of 185 ± 62 MBq. Whole-body PET scans were obtained using 4–5 bed positions (depending on patient size) at an acquisition time of 8 min each, covering the skull base to mid thighs. PET images were reconstructed using iterative ordered-subset expectation maximization with 3 iterations and 21 subsets, a gaussian filter of 4 mm in full width at half maximum, and a 344 × 344 matrix. The PET data were automatically attenuation-corrected using a 4-compartment-model attenuation map calculated from fat-only and water-only images as obtained from Dixon-based sequences. MR imaging data were acquired simultaneously with a dedicated mMR head and neck coil and phased-array body surface coils using the following whole-body imaging protocol: a coronal 3-dimensional volume-interpolated breath-hold examination (VIBE) sequence (repetition time [TR], 3.6 ms; first echo time [TE], 1.23 ms; second TE, 2.46 ms; slice thickness, 3.12 mm; field of view [FOV], 500 mm) for Dixon-based attenuation correction; a transversal echoplanar DWI sequence (TR, 9,900 ms; TE, 55 ms; diffusion weighting (b-values), 0, 500, and 1,000 s/mm^2; matrix, 160; slice thickness, 5 mm; FOV, 420 mm); a coronal 2-dimensional turbo inversion recovery magnitude sequence (TR, 3,190 ms; TE, 55 ms; matrix, 384; slice thickness, 5 mm; FOV, 450 mm); a transversal 2-dimensional fat-saturated half-Fourier acquisition single-shot turbo spin echo sequence (TR, 1,500 ms; TE, 117 ms; matrix, 320; slice thickness, 5 mm; FOV, 450 mm); and a transversal 3-dimensional postcontrast VIBE sequence (TR, 4.08 ms; TE, 1.51 ms; matrix, 512; slice thickness, 3.5 mm; FOV, 400 mm). The dedicated pelvic MR imaging protocol consisted of a transversal 3-dimensional VIBE sequence (TR, 4.46 ms; TE, 1.71 ms; matrix, 512; slice thickness, 2.5 mm; FOV, 300 mm) and a sagittal turbo spin echo sequence (TR, 4,440 ms; TE, 101 ms; matrix, 512; slice thickness, 4.0 mm; FOV, 280 mm). Additionally, a sagittal 3-dimensional VIBE sequence (TR, 4.46 ms; TE, 1.71 ms; matrix, 512; slice thickness, 2.5 mm; FOV, 300 mm) and, for dynamic imaging, 3 repetitive scans were acquired at a delay of 20, 60, and 90 s after intravenous administration of gadobutrol (Gadovist; Bayer HealthCare) (0.1 mmol/kg of body weight).

Image Analysis

Two radiologists with 6 and 9 y of experience in interpreting MR imaging and hybrid imaging, respectively, rated the images separately in random order using dedicated viewing software for integrated imaging (Syngo.via; Siemens Healthcare). Patient- and lesion-based image analysis was performed in 2 sessions separated by a minimum of 4 wk to avoid recognition bias. The first session comprised interpretation of the PET/MR imaging datasets alone. In the second session, PET/MR imaging data including DWI were assessed. Both readers were masked to patient identification data and diagnosis and were asked to identify all primary tumors, as well as lymph node and distant metastases. Malignancy was considered if 1 of the 3 following criteria was deemed positive: (a) Morphology: Primary tumors (local tumor invasion, contrast enhancement, central necrosis); lymph nodes (maximum diameter in short axis > 10 mm, shape (smooth vs. irregular), distinctive contrast enhancement, central necrosis); distant metastases (distinctive contrast enhancement, central necrosis), (b) ^{18}F-FDG avidity: focally increased ^{18}F-FDG uptake, (c) Diffusion-restriction: high signal intensity in DWI (b-1000 s/mm^2) and low signal in corresponding ADC map.

Furthermore, the size of primary tumors and metastases was measured. To quantify the metabolic activity of ^{18}F-FDG–avid lesions, maximum and mean standardized uptake values (SUV_{max} and SUV_{mean}, respectively) were determined by drawing a 3-dimensional isocontour on PET/MR images, which helped provide orientation for characterizing findings as benign or malignant. With DWI as a part of the PET/MR imaging protocols, lesions in our study were classified on the basis of visual criteria (high signal in b-1000 with a signal drop in the corresponding ADC parameter map). In a further session, both readers qualitatively assessed the PET and DWI data. All lesions were graded for conspicuity (visual lesion-to-background contrast; 1, not visible; 2, low contrast; 3, moderate contrast; 4, high contrast) and diagnostic confidence (1, not confident; 2, confident; 3, very confident).

Reference Standard

Malignant disease was confirmed histopathologically in all 27 patients with primary tumors and in 12 patients with recurrence of a pelvic malignancy. In the remaining 9 patients, tumor relapse was not confirmed histopathologically, because current guidelines do not call for surgery or histopathologic confirmation in recurrences of specific cancer types. (*13,14*). Therefore, when histopathologic confirmation was not available, only patients with an imaging follow-up of at least 6 mo were included. In accordance with previous publications evaluating the diagnostic capacity of PET/MR imaging for tumor detection, the reference standard consisted of a consensus interpretation for each lesion based on all available histopathologic samples, prior examinations, PET/CT, PET/MR imaging, cross-sectional follow-up imaging (mean ± SD, 345 ± 155 d; range, 187–679), and clinical follow-up (*15,16*). Correspondingly, a suggestive lesion was considered malignant when it disappeared, grew smaller, or showed decreasing ^{18}F-FDG

TABLE 1
Distribution of Patients According to Diagnosis, Subdivided into Primary and Recurrent Cancer

Diagnosis	No. of patients with…	
	Primary cancer	Recurrent cancer
Cervical cancer	17	5
Vulvar cancer	7	1
Vaginal cancer	2	3
Endometrial cancer	1	3
Ovarian cancer	—	9
Total ($n = 48$)	27	21

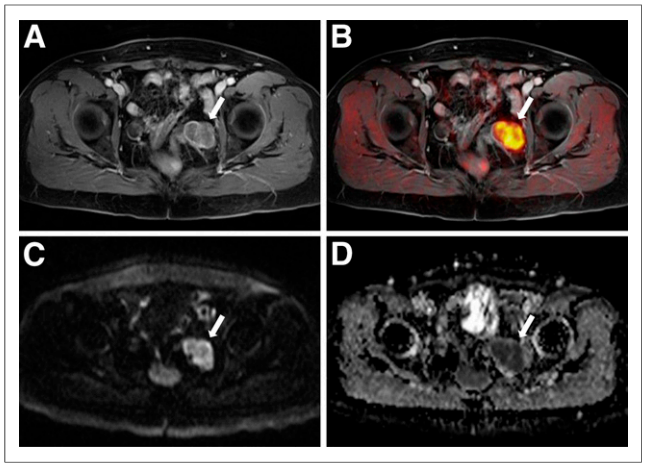

FIGURE 1. Images of 51-y-old patient with recurrence of ovarian cancer (arrows). Contrast-enhanced MR image (A) shows tumor on left side of pelvis; tumor has focally increased tracer uptake on PET/MR imaging (B). The same lesion has high signal intensity (b-1000) on DWI (C) and low signal intensity on corresponding ADC map (D).

accumulation under systemic therapy and when an increase or decrease in number and size of lesions was seen in subsequent examinations. Conversely, morphologically inconspicuous and PET-negative lesions on PET/MR imaging and imaging follow-up examinations were considered benign.

Statistical Analysis

SPSS, version 21 (IBM), was used for statistical analysis. Data are presented as mean ± SD. Descriptive analysis was used to evaluate the resulting scores. The Wilcoxon signed-rank test was used to indicate potential significant differences between PET and DWI datasets. The sensitivity, specificity, positive predictive value, negative predictive value, and diagnostic accuracy for PET/MR imaging alone and PET/MR imaging including DWI were calculated, and the McNemar test was used to determine the significance of differences between the 2 ratings. *P* values of less than 0.05 were considered statistically significant.

RESULTS

Patients

PET/MR imaging examinations were successfully completed for all 48 patients with primary ($n = 27$) or potentially recurrent ($n = 21$) pelvic malignancies, without any relevant side effects (Table 1). The examination time averaged 41 ± 4 min, including patient positioning, scan planning, breath-hold commands, contrast administration, and data acquisition. The DWI acquisition time ranged from 11 to 14 min for 4–5 bed positions.

Malignant lesions were found in 41 (85.4%) of the 48 patients. In the remaining 7 patients, no tumor recurrence was found on PET/MR imaging or subsequent follow-up examinations.

Lesion Detection

A total of 122 suspected lesions were seen, with 98 lesions considered malignant according to the reference standard (Fig. 1). Primary tumors and metastases had a mean size of 3.7 ± 2.0 cm and 1.5 ± 0.8 cm, respectively; a mean SUV_{max} of 13.2 ± 6.3 and 7.7 ± 4.3, respectively; and a mean SUV_{mean} of 6.5 ± 3.2 and 4.1 ± 2.2, respectively. PET/MR imaging alone correctly detected 91 of the 98 lesions, for a sensitivity of 92.9%, specificity of 87.5%, positive predictive value of 96.8%, negative predictive value of 75.0%, and accuracy of 91.8% (Table 2). Including DWI in PET/MR imaging protocols allowed 2 additional lesions (93/98) to be correctly detected on the basis of restricted diffusivity on DWI and a signal drop on the corresponding ADC maps, resulting in slightly but not significantly higher values (94.9%, 83.3%, 95.9%, 80.0%, and 92.6%, respectively; $P > 0.05$) with no associated changes in therapy management. The 2 additionally detected metastases had no morphologic or metabolic characteristics suggestive of malignancy based on PET/MR imaging alone (Fig. 2) but were determined to be cancer lesions because of histopathologic confirmation (lymph node metastasis) and cross-sectional imaging follow-up (peritoneal lesion).

Furthermore, according to both interpretations (PET/MR imaging with and without DWI), 3 of 22 benign lesions were misclassified as malignant (Table 3). Among them, 1 pulmonary lesion in the right upper lobe (11 mm along the long axis) showed focally increased uptake (SUV_{max}, 2.9) and restricted diffusivity but was histopathologically confirmed as localized organizing pneumonia after segmentectomy (Fig. 3). Two lymph nodes (7 and 9 mm) showed focally increased metabolic activity and restricted diffusivity but were determined to be benign on the basis of histopathologic sampling after lymphadenectomy. One additional lymph node did not show clear signs of malignancy based on morphologic and metabolic criteria (SUV_{max}, 1.8) but was rated false-positive on PET/MR imaging with DWI because of suggestive characteristics on DWI.

Lesion Conspicuity and Diagnostic Confidence

Of the 98 detected malignant lesions, 7 (7.1%) did not have a high signal intensity on the DWI images (b-1000) or a signal drop on the corresponding ADC maps. Among them, 1 primary cervical cancer lesion, 1 bone metastasis, and 1 additional lymph node metastasis did not have elevated tracer accumulation and could not

TABLE 2
Detection of Malignant Lesions on PET/MR Imaging With or Without DWI

Modality	Primary tumor site	Lymph nodes	Peritoneal lesions	Liver	Bone	Lung	Total
Without DWI							
True-positive	29 (29.6%)	36 (36.7%)	14 (14.3%)	7 (7.1%)	2 (2.0%)	3 (3.1%)	91 (92.9%)
False-negative	1 (1.0%)	4 (4.1%)	1 (1.0%)	—	1 (1.0%)	—	7 (7.1%)
With DWI							
True-positive	29 (29.6%)	37 (37.8%)	15 (15.3%)	7 (7.1%)	2 (2.0%)	3 (3.1%)	93 (94.9%)
False-negative	1 (1.0%)	3 (3.1%)	—	—	1 (1.0%)	—	5 (5.1%)
All lesions	30 (30.6%)	40 (40.8%)	15 (15.3%)	7 (7.1%)	3 (3.1%)	3 (3.1%)	98 (100%)

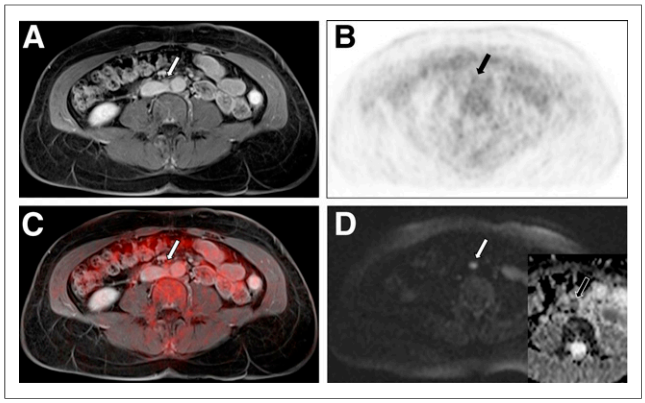

FIGURE 2. Images of 57-y-old patient with paraaortic lymph node metastasis of cervical cancer (arrows). Contrast-enhanced MR image (A) shows morphologically inconspicuous lymph node (6 mm along short axis). PET (B) does not reveal focally increased tracer accumulation; accordingly, node was rated as benign on PET/MR imaging (C). DWI (D) shows high signal intensity (b-1000) with signal drop in corresponding ADC map (inset), leading to correct identification of lymph node metastasis on PET/MR-with-DWI rating.

be delineated on PET images. Therefore, qualitative assessment of lesion-to-background contrast for both functional parameters revealed significantly ($P < 0.05$) higher values for PET than for DWI (Table 4). When diagnostic confidence was compared between PET and DWI, PET had significantly ($P < 0.05$) higher scores for the determination of malignant lesions (Table 5).

DISCUSSION

The present study investigating the diagnostic value of DWI in PET/MR imaging protocols for whole-body staging of women with pelvic malignancies delivered 2 important messages. First, the inclusion of DWI in PET/MR imaging protocols did not significantly increase the detection rate of malignant lesions or improve false-negative ratings. Second, when the 2 functional parameters were compared, PET had significantly higher lesion-to-background contrast and higher diagnostic confidence in the assessment of malignant lesions than DWI.

High-quality staging and restaging of cancer patients is essential to enable the best possible management and depends on high-quality imaging techniques. The evaluation of potentially increased metabolic activity on ^{18}F-FDG PET has been shown to be highly valuable for detection of tumors (*17,18*). Yet, adding morphologic information to the metabolic data is considered beneficial for counteracting potential false-negative PET findings based on the low spatial resolution of PET (<10 mm) or ^{18}F-FDG tumors with little to no avidity (*19,20*). Hence, the establishment of integrated imaging techniques such as PET/CT scanners, combining functional and high-resolution anatomic information, set a new milestone for whole-body tumor staging (*6,21*). Despite the excellent diagnostic accuracy of PET/CT in comparison to other conventional imaging techniques that have a reasonable scan duration, the CT component is limited by the ionizing radiation and low soft-tissue contrast. Hence, the introduction of PET/MR imaging scanners, using MR imaging for the morphologic component, enables a combination of high-quality morphologic imaging with excellent soft-tissue contrast and the diagnostic advantages of PET while reducing ionizing radiation exposure. Numerous oncology studies have shown the high diagnostic value of PET/MR imaging, which is comparable and sometimes superior to PET/CT in dedicated applications (e.g., detection of liver metastases) (*15,22,23*). However, the long acquisition times of PET/MR imaging, caused mainly by the application of various MR sequences, can cause patient discomfort. Hence, a dedicated evaluation of the true diagnostic benefit of dedicated sequences is needed to further establish the merits of PET/MR imaging for clinical oncologic imaging (*24*). Despite the proven benefits of adding DWI to conventional MR imaging, the added value for PET/MR imaging has been debatable based on initial results from small patient cohorts (*16,25, 26*). After viewing these initial results, we decided to amplify the patient cohort and evaluate the diagnostic impact of diffusion-weighted sequences as a part of a standardized whole-body MR protocol for staging and restaging gynecologic malignancies. Our results underline the questionable diagnostic benefit of the inclusion of DWI, as a comparison of PET/MR imaging with and without DWI yielded comparable values for sensitivity, specificity, positive predictive value, negative predictive value, and accuracy. The only added benefit based on DWI was the detection of 2 metastases exhibiting high signal intensity on DWI (b-1000) and a signal drop on the corresponding ADC map yet not having any morphologic characteristics of malignancy or an increased ^{18}F-FDG avidity. However, the detection of these 2 lesions did not result in significant changes in sensitivity or specificity or a change in patient management. Qualitative assessments showed that, compared with DWI, PET had significantly higher lesion contrast and higher values for diagnostic confidence in the detection of malignant lesions. Furthermore, our ratings for PET/MR imaging alone and PET/MR imaging with DWI resulted in 3 identical false-positive findings, with 2 lymph nodes and 1 lung lesion showing morphologic or functional signs of malignancy. One additional lymph node

TABLE 3
Localization and Characterization of Benign Lesions on PET/MR Imaging With or Without DWI

Modality	Primary tumor site	Lymph nodes	Peritoneal lesions	Liver	Bone	Lung	Total
Without DWI							
True-negative	4 (16.7%)	6 (25.0%)	1 (4.2%)	7 (29.2%)	1 (4.2%)	2 (8.3%)	21 (87.5%)
False-positive	—	2 (8.3%)	—	—	—	1 (4.2%)	3 (12.5%)
With DWI							
True-negative	4 (16.7%)	5 (20.8%)	1 (4.2%)	7 (29.2%)	1 (4.2%)	2 (8.3%)	20 (83.3%)
False-positive	—	3 (12.5%)	—	—	—	1 (4.2%)	4 (16.7%)
All lesions	4 (16.7%)	8 (33.3%)	1 (4.2%)	7 (29.2%)	1 (4.2%)	3 (12.5%)	24 (100%)

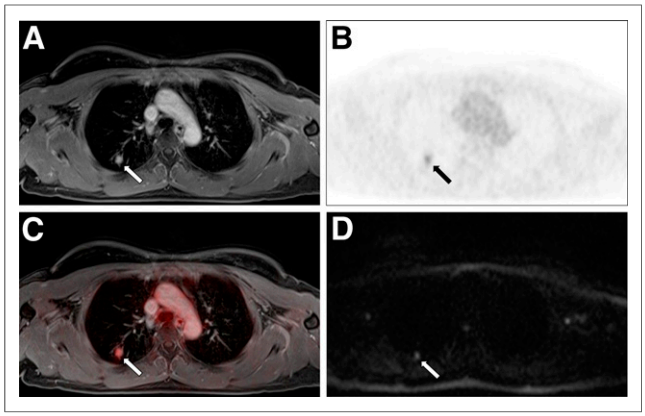

FIGURE 3. Images of 50-y-old patient with primary cervical cancer and 11-mm mass in right upper lobe of lung (arrows) on contrast-enhanced MR image (A), revealing focal tracer uptake on PET (B) and PET/MR imaging (C) and restricted diffusivity (D, b-1000). Hence, lesion was considered malignant in both ratings (PET/MR imaging with or without DWI). According to histopathologic work-up after segmental resection, lesion was considered to be organizing pneumonia.

was rated false-positive on PET/MR imaging with DWI on the basis of suggestive characteristics on DWI.

Our study results are in line with the results of previous studies assessing the diagnostic benefit of adding DWI to PET/MR imaging. Buchbender et al. published their first results on efficient scan protocols, assessing 5 primary tumors and 44 metastases (*16*). All 49 lesions were concordantly detected by ^{18}F-FDG PET/MR imaging with or without DWI, with lesion-to-background contrast being better for PET than for DWI. Investigating subsequent PET/MR imaging with or without DWI for cervical lymph node metastases, Heusch et al. found no significant differences in diagnostic accuracy between PET/MR imaging with DWI and PET/MR imaging without DWI, despite the disadvantage that the PET and MR imaging datasets had been fused retrospectively (coregistration artifacts, different patient positioning in the 2 imaging sessions) (*25*). With simultaneous PET/MR imaging being a novel technique, few studies have investigated it. Comparing the diagnostic accuracy of whole-body DWI and MR imaging with that of PET/CT for tumor staging, Michielsen et al. reported an equivalent diagnostic accuracy for characterization of primary ovarian cancers and detection of lymph nodes and distant metastases yet also revealed the superiority of DWI and MR imaging for detecting and characterizing peritoneal lesions (*9*). Similar results were shown by Soussan et al., who found that DWI and MR imaging are superior to PET/CT for detecting peritoneal implants in the right supramesocolic area (*7*). This result was due mainly to physiologic uptake in the adjacent liver tissue and respiratory motion artifacts, leading to underestimation of uptake in metastatic sites on PET. These study results agree with ours in that they show the high diagnostic ability of PET/MR imaging and PET/CT and the only minor benefit from adding DWI. Nevertheless, the diagnostic competence of exclusive PET/MR imaging depends on the tracer avidity of potential tumors. Hence, in investigations of less ^{18}F-FDG–avid tumor types (e.g., hepatocellular carcinomas) or specific body regions, the use of DWI in PET/MR imaging might have greater value in oncologic work-ups and should be evaluated in future studies.

TABLE 4
Resulting Scores for Contrast of Malignant Lesions on PET Versus DWI

Modality	PET	DWI
Mean ± SD	3.8 ± 0.7	3.6 ± 0.8
Median	4 (range, 1–4)	4 (range, 1–4)

TABLE 5
Diagnostic Confidence of PET Versus DWI for Evaluation of Malignant Lesions

Modality	PET	DWI
Mean ± SD	2.7 ± 0.6	2.5 ± 0.7
Median	3 (range, 1–3)	3 (range, 1–3)

Our study was not free of limitations. To our knowledge, the enrolled number of patients in this study was the largest with gynecologic malignancies yet studied by PET/MR imaging. However, our results should be considered preliminary and open to further confirmation in future studies with larger cohorts. Another limitation was the restricted reference standard. Histopathologic sampling of all suspected lesions would have been desirable to provide a clean reference standard. However, current guidelines (*13,14*) and clinical patient management do not require histopathologic sampling of all suggestive lesions in order to initiate appropriate patient management and therapy. Therefore, in accordance with previous publications on PET/MR imaging, we used all applicable histopathologic results and cross-sectional imaging follow-up results as the reference standard (*15,16*).

CONCLUSION

Our study showed the high diagnostic potential of PET/MR imaging for staging and restaging women with pelvic malignancies but did not show a clear diagnostic benefit from including DWI. Hence, the omission of DWI may help optimize PET/MR imaging protocols for ^{18}F-FDG–avid gynecologic malignancies by reducing scan duration and improving patient comfort.

REFERENCES

1. Bipat S, Glas AS, van der Velden J, Zwinderman AH, Bossuyt PM, Stoker J. Computed tomography and magnetic resonance imaging in staging of uterine cervical carcinoma: a systematic review. *Gynecol Oncol.* 2003;91:59–66.
2. Alvarez Moreno E, Jimenez de la Pena M, Cano Alonso R. Role of new functional MRI techniques in the diagnosis, staging, and followup of gynecological cancer: comparison with PET-CT. *Radiol Res Pract.* 2012;2012:219546.
3. Low RN, Sebrechts CP, Barone RM, Muller W. Diffusion-weighted MRI of peritoneal tumors: comparison with conventional MRI and surgical and histopathologic findings—a feasibility study. *AJR.* 2009;193:461–470.
4. Kuang F, Ren J, Zhong Q, Liyuan F, Huan Y, Chen Z. The value of apparent diffusion coefficient in the assessment of cervical cancer. *Eur Radiol.* 2013;23:1050–1058.
5. Chen YB, Hu CM, Chen GL, Hu D, Liao J. Staging of uterine cervical carcinoma: whole-body diffusion-weighted magnetic resonance imaging. *Abdom Imaging.* 2011;36:619–626.
6. Antoch G, Saoudi N, Kuehl H, et al. Accuracy of whole-body dual-modality fluorine-18-2-fluoro-2-deoxy-D-glucose positron emission tomography and computed tomography (FDG-PET/CT) for tumor staging in solid tumors: comparison with CT and PET. *J Clin Oncol.* 2004;22:4357–4368.

7. Soussan M, Des Guetz G, Barrau V, et al. Comparison of FDG-PET/CT and MR with diffusion-weighted imaging for assessing peritoneal carcinomatosis from gastrointestinal malignancy. *Eur Radiol.* 2012;22:1479–1487.
8. Mayerhoefer ME, Karanikas G, Kletter K, et al. Evaluation of diffusion-weighted MRI for pretherapeutic assessment and staging of lymphoma: results of a prospective study in 140 patients. *Clin Cancer Res.* 2014;20:2984–2993.
9. Michielsen K, Vergote I, Op de Beeck K, et al. Whole-body MRI with diffusion-weighted sequence for staging of patients with suspected ovarian cancer: a clinical feasibility study in comparison to CT and FDG-PET/CT. *Eur Radiol.* 2014;24: 889–901.
10. Grueneisen J, Beiderwellen K, Heusch P, et al. Simultaneous positron emission tomography/magnetic resonance imaging for whole-body staging in patients with recurrent gynecological malignancies of the pelvis: a comparison to whole-body magnetic resonance imaging alone. *Invest Radiol.* July 9, 2014 [Epub ahead of print].
11. Vargas MI, Becker M, Garibotto V, et al. Approaches for the optimization of MR protocols in clinical hybrid PET/MRI studies. *MAGMA.* 2013;26:57–69.
12. Wetter A, Lipponer C, Nensa F, et al. Simultaneous ^{18}F choline positron emission tomography/magnetic resonance imaging of the prostate: initial results. *Invest Radiol.* 2013;48:256–262.
13. Wagner U, Harter P, Hilpert F, et al. S3-guideline on diagnostics, therapy and follow-up of malignant ovarian tumours: short version 1.0 - AWMF registration number: 032/035OL, June 2013. *Geburtshilfe Frauenheilkd.* 2013;73:874–889.
14. Beckmann MW, Mallmann P. Interdisciplinary S2k guideline on the diagnosis and treatment of cervical carcinoma. *J Cancer Res Clin Oncol.* 2009;135:1197–1206.
15. Beiderwellen K, Gomez B, Buchbender C, et al. Depiction and characterization of liver lesions in whole-body [^{18}F]-FDG PET/MRI. *Eur J Radiol.* 2013;82: e669–e675.
16. Buchbender C, Hartung-Knemeyer V, Beiderwellen K, et al. Diffusion-weighted imaging as part of hybrid PET/MRI protocols for whole-body cancer staging: does it benefit lesion detection? *Eur J Radiol.* 2013;82:877–882.
17. AAssar OS, Fischbein NJ, Caputo GR, et al. Metastatic head and neck cancer: role and usefulness of FDG PET in locating occult primary tumors. *Radiology.* 1999;210:177–181.
18. Havrilesky LJ, Kulasingam SL, Matchar DB, Myers ER. FDG-PET for management of cervical and ovarian cancer. *Gynecol Oncol.* 2005;97:183–191.
19. Yamazaki Y, Saitoh M, Notani K, et al. Assessment of cervical lymph node metastases using FDG-PET in patients with head and neck cancer. *Ann Nucl Med.* 2008;22:177–184.
20. Kitajima K, Murakami K, Yamasaki E, et al. Performance of integrated FDG-PET/contrast-enhanced CT in the diagnosis of recurrent uterine cancer: comparison with PET and enhanced CT. *Eur J Nucl Med Mol Imaging.* 2009;36: 362–372.
21. Beyer T, Townsend DW, Brun T, et al. A combined PET/CT scanner for clinical oncology. *J Nucl Med.* 2000;41:1369–1379.
22. Kubiessa K, Purz S, Gawlitza M, et al. Initial clinical results of simultaneous ^{18}F-FDG PET/MRI in comparison to ^{18}F-FDG PET/CT in patients with head and neck cancer. *Eur J Nucl Med Mol Imaging.* 2014;41:639–648.
23. Pace L, Nicolai E, Luongo A, et al. Comparison of whole-body PET/CT and PET/MRI in breast cancer patients: lesion detection and quantitation of ^{18}F-deoxyglucose uptake in lesions and in normal organ tissues. *Eur J Radiol.* 2014; 83:289–296.
24. Martinez-Möller A, Eiber M, Nekolla SG, et al. Workflow and scan protocol considerations for integrated whole-body PET/MRI in oncology. *J Nucl Med.* 2012;53:1415–1426.
25. Heusch P, Sproll C, Buchbender C, et al. Diagnostic accuracy of ultrasound, ^{18}F-FDG-PET/CT, and fused ^{18}F-FDG-PET-MR images with DWI for the detection of cervical lymph node metastases of HNSCC. *Clin Oral Investig.* 2014;18:969–978.
26. Thoeny HC, Forstner R, De Keyzer F. Genitourinary applications of diffusion-weighted MR imaging in the pelvis. *Radiology.* 2012;263:326–342.